Reconstruction of Power Lines from Point Clouds

Alexander Gribov* and Khalid Duri†
Esri
380 New York Street, Redlands, CA 92373-8100, USA
*agribov@esri.com, †kduri@esri.com

arXiv:2201.12499v1 [cs.CV] 29 Jan 2022

Abstract

This paper proposes a novel solution for constructing line features modeling each catenary curve present within a series of points representing multiple catenary curves. The solution can be applied to extract power lines from lidar point clouds, which can then be used in downstream applications like creating digital twin geospatial models and evaluating the encroachment of vegetation. This paper offers an example of how the results obtained by the proposed solution could be used to assess vegetation growth near transmission power lines based on freely available lidar data for the City of Utrecht, Netherlands [1].

Index Terms

Lidar Point Cloud; Power Lines; Digital Twin; Vegetation Encroachment; Catenary Curve Fitting; Finding Closest Point

I. Introduction

This paper proposes a novel solution of constructing line features modeling each catenary curve that is present within a series of points representing multiple catenary curves. Utility companies can leverage this solution to extract power lines from lidar surveys and identify specific attributes. The extracted power lines can be used to assess the locational accuracy of the power lines and determine whether the amount of sag (see calculation of sag in [2]) indicates any need for maintenance of the support structure. Additionally, the extracted power lines can be incorporated into downstream operations like mitigating fire risk from vegetation encroachment. The power lines can help define the vegetation clearance zone surrounding them, as demonstrated later in this paper. The importance of maintaining power lines and their surrounding vegetation was underscored by the spate of fires in California caused by power lines (see Table I). Of the fires related to power lines in 2020, vegetation contact accounted for nearly 93 percent of the area damaged [3].

Table I: History of California wildfires caused by power lines. [3]–[6]

Year	Incident count	Incident count of acres burned ≥ 10	Acres burned	Dollar damage	% of total burned area
2020	335	31	59,334	$\$52,001,282$[1]	4%
2019	304	37	83,729	$\$388,843,293$	65%
2018	297	26	246,873	$\$2,001,803,168$	23%
2017	408	65	249,501	$\$12,046,544,839$	53%

Lidar provides a cost-effective solution for surveying the location of power lines and other objects of interest with great measures of accuracy. The points obtained from a lidar survey can be classified using a variety of techniques—from deterministic, rule-based operations and manual editing to deep learning. Once the points from power lines are classified, they can be processed with the proposed solution to produce a polyline representation for each power line. The resultant polylines can overcome gaps in the lidar survey and ensure the connectivity of each power line span.

The approach can be summarized as follows:

1. Use the minimum spanning tree clustering algorithm to connect points and cut them into sequences of *combined* points (Section II).
2. Apply the dynamic programming approach to ensure the separation of each catenary curve (Section III). The dynamic programming approach uses a penalty function based on fitting the catenary curve to points (Section V).
3. Use the k-mean clustering algorithm to improve partitioning. In k-mean iterative steps, the update step refits catenary curves to the newly found clusters (Section V) and the assignment step uses the algorithm to find the closest points along the catenary curves (Section IV).

An example of the solution is shown in Section VI.

[1]Fires from undetermined causes resulted in $\$2,121,798,631$ in damages.

II. Clustering Catenary Curves

Let's define a combined point as a nonempty set of points and a combined polyline as a list of combined points. A combined polyline is considered small if it contains no more than the predetermined minimum number of combined points, and it is not small if it has more combined points than the predetermined maximum number of points. The prolongated form is discovered for all combined polylines whose points are in the range of the predetermined minimum and maximum number of points. This form is found by evaluating the ratio of the median axis to the largest axis of the ellipse constructed from the covariance matrix of the coordinates for each point in the combined polyline. This will be used to evaluate whether the predetermined threshold value has been exceeded.

The steps of the algorithm are the following:

1. For the source points, apply the minimum spanning tree (MST) clustering algorithm using edges whose length does not exceed the user-specified threshold for the maximum allowed gap. See algorithms for the minimum spanning tree in [7]–[10]. Note the following: *"Out of many available algorithms to solve MST, the Borůvka's algorithm is the basis of the fastest known algorithms"* [11].
2. Assign each node of the network to an empty set of combined polylines.
3. Store all nonsmall combined polylines for each end node with more than one nonsmall combined polyline, and discard all other combined polylines. Add the empty combined polyline to the neighboring node. To prevent merging combined polylines through this node, mark that empty combined polyline as not small. Perform the following for all other end nodes:
   a. Find the longest combined polylines by the number of combined points, giving preference to nonsmall combined polylines.
   b. If there is only one longest combined polyline, take all points from other combined polylines, add these points and the node point as a combined point to the longest combined polyline, and add this modified combined polyline to the neighboring node.
   c. When two are the longest, construct a new combined polyline with a combined point containing all points from all combined polylines in the node and the node point, and add this combined polyline to the neighboring node.
4. Delete all processed end nodes and go to step 3 unless no end nodes remain.
5. Note that at this stage, all nodes are isolated. Next, store all nonsmall combined polylines for each node with more than two nonsmall combined polylines. Otherwise, merge nonsmall combined polylines through the combined point with all points from other combined polylines and the node point.
6. For all stored combined polylines, apply the division algorithm described in Section III.
7. Use the partitioning in the previous step as a starting solution for the k-mean clustering algorithm [12]. The k-mean clustering algorithm is then applied by alternating steps for fitting catenary curves to points and reallocating points to the closest catenary curves. Also, an essential intermediate step is merging similar catenary curves.

This approach results in the identification of all points that belong to the same catenary curve. Consideration must be taken for the density of the points and expected length of the nominal catenary curve when determining appropriate values for the minimum and maximum number of points.

III. Dividing a Combined Polyline

The task is to find the optimal division of a combined polyline such that it minimizes the number of partitions and the penalty in each partition. In other words, each partition should have the best fit while encouraging the division of partitions when the fit improves significantly.

We found the following empirical penalties for each partition:

$$-\frac{\sum \epsilon_i^2}{2 \cdot n \cdot T^2},$$

where ϵ_k is the deviation from the fitted catenary curve, n is the number of points in the partition, and T is the maximum deviation from the catenary curve specified by the user. Fitting is performed without removing any points even if they violate the maximum deviation. Also, all points in a combined point cannot be divided.

And for the partitions not larger than the predetermined number of points, the penalty is

$$\log\left(\frac{1}{2}\right),$$

plus the total number of partitions times $\log\left(\frac{1}{2}\right)$.

From a probabilistic point of view, this penalty formulation can be treated in the following way:

- Each partition has a probability
$$\mathrm{f}_{exp}\left(\frac{\sum \epsilon_i^2}{2 \cdot n \cdot T^2}\right),$$
where f_{exp} is the probability density function of the exponential distribution with an intensity equal to 1
$$\mathrm{f}_{exp}(x) = \begin{cases} e^{-x}, & x \geq 0, \\ 0, & \text{otherwise.} \end{cases}$$
- And for the partitions not larger than the user-specified number of points, the probability is $\frac{1}{2}$. The probability for each partition is $\frac{1}{2}$, or in other words, the probability to have extra partition is $\frac{1}{2}$ and the probability not to have any more partitions is $\frac{1}{2}$. Therefore, the number of partitions follows the geometric distribution with probability equaling $\frac{1}{2}$.

The total probability is equal to the product of probabilities.

To find the optimal division, we use the dynamic programming approach described in [13].

IV. Finding the Closest Point on the Catenary Curve

The catenary curve equation is
$$y = c + a \cdot \cosh\left(\frac{x-m}{a}\right). \tag{1}$$

Finding the point C on the catenary curve closest to some point A in three-dimensional space is the same as finding the point C on the catenary curve closest to the point B, where B is a projection of point A onto the catenary curve's plane—see Figure 1. Because point B is a projection of point A onto the catenary curve's plane and point C is the closest point to point B, it follows that point A is located on the tangent plane of the catenary curve constructed at point C. Therefore, finding the closest point in three-dimensional space can be done by projecting the point onto the catenary curve's plane, then determining the closest point on the catenary curve for the projected point.

To find the point closest to point $\mathbf{p} = \begin{bmatrix} x_p \\ y_p \end{bmatrix}$ on the catenary curve defined by (1), we first apply the coordinate system's transformation:
$$\begin{aligned} x' &= \frac{x-m}{a}, \\ y' &= \frac{y-c}{a}. \end{aligned}$$

After this transformation, the catenary curve (1) becomes
$$y' = \cosh(x'), \tag{2}$$
and point $\mathbf{p}$ transforms to $\mathbf{p}' = \begin{bmatrix} x'_p \\ y'_p \end{bmatrix}$, where
$$\begin{aligned} x'_p &= \frac{x_p-m}{a}, \\ y'_p &= \frac{y_p-c}{a}. \end{aligned}$$

Because this transformation is translation and dilation, it follows that if the point $\mathbf{p}'_c = \begin{bmatrix} x'_c \\ y'_c \end{bmatrix}$ on the catenary curve (2) closest to the point is $\mathbf{p}'$, then $\mathbf{p}_c = \begin{bmatrix} x_c \\ y_c \end{bmatrix}$, where
$$\begin{aligned} x_c &= a \cdot x'_c + m, \\ y_c &= a \cdot y'_c + c \end{aligned}$$
is the location on the catenary curve (1) closest to the point $\mathbf{p}$.

Therefore, without loss of generality, it is sufficient to solve the task of finding the closest point on the catenary curve (1) by considering only the case when $a = 1$, $m = 0$, and $c = 0$; therefore, we will refer to the catenary curve as a function:
$$y = \cosh(x).$$

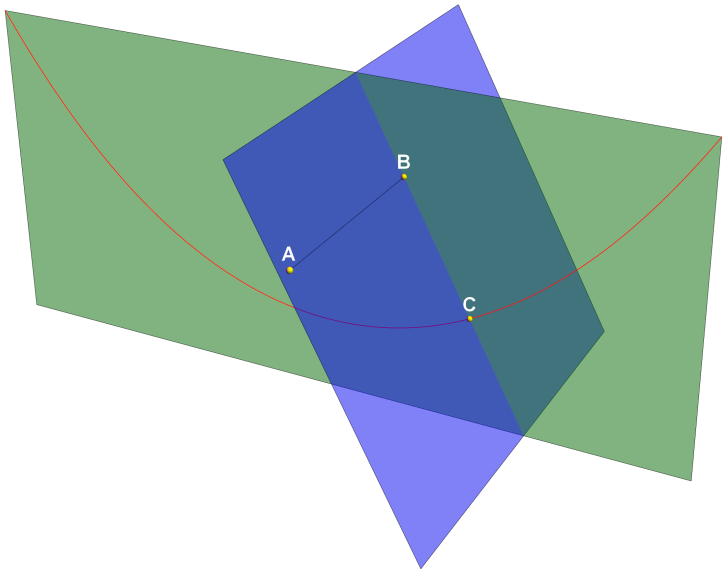


Figure 1: The catenary curve (red line) is defined in a plane (green). Point B is a projection of point A into the catenary curve's plane. Point C is the point on the catenary curve closest to point B. The tangent plane (blue) for the catenary curve is constructed for point C.

The derivative at point x is $\sinh(x)$, and it is strictly an increasing function. The normal to the catenary curve is $\begin{bmatrix} \tanh(x) \\ -\operatorname{sech}(x) \end{bmatrix}$ (see Figure 2), and it will intersect the y-axis at

$$y = \cosh(x) + \frac{x}{\sinh(x)}. \tag{3}$$

Equation (3) is an even function, strictly increasing for positive x, and strictly decreasing for negative x; see proof in Appendix I. From these properties, it follows that the closest point is unique for any location except the line from point $\begin{bmatrix} 0 \\ 2 \end{bmatrix}$ to $\begin{bmatrix} 0 \\ +\inf \end{bmatrix}$, shown in blue. While the point $\begin{bmatrix} 0 \\ 2 \end{bmatrix}$ has a unique closest point $\begin{bmatrix} 0 \\ 1 \end{bmatrix}$, all other points on the blue line have two equally distant closest points. There is an area of numerical instability for finding the closest point for points close to the point $\begin{bmatrix} 0 \\ 2 \end{bmatrix}$. In this paper, for all points on the line from point $\begin{bmatrix} 0 \\ 2 \end{bmatrix}$ to $\begin{bmatrix} 0 \\ +\inf \end{bmatrix}$ and around point $\begin{bmatrix} 0 \\ 2 \end{bmatrix}$, point $\begin{bmatrix} 0 \\ 1 \end{bmatrix}$ will be assigned as the closest.

Let's start by partitioning the area by normal lines from the catenary curve. Without loss of generality, it is sufficient to consider only half of the plane $x > 0$. Choosing $x_i = k \cdot i$, $i \in \mathbb{N}_0$, construct lines passing through points $\begin{bmatrix} x_i \\ \cosh(x_i) \end{bmatrix}$ with directions $\begin{bmatrix} \tanh(x_i) \\ -\operatorname{sech}(x_i) \end{bmatrix}$. The example of partitioning the area for the case when $k = \frac{1}{4}$ is shown in Figure 2.

Finding the partition is performed by a binary search. The bounds can be narrowed by finding the intersection of horizontal and vertical lines drawn from the point $\mathbf{p}$ with the catenary curve.

While this algorithm can be used for finding the catenary curve's closest point by subdividing on each iteration, many steps are needed to converge. However, if performance is not a concern, it can be the chosen algorithm for this task.

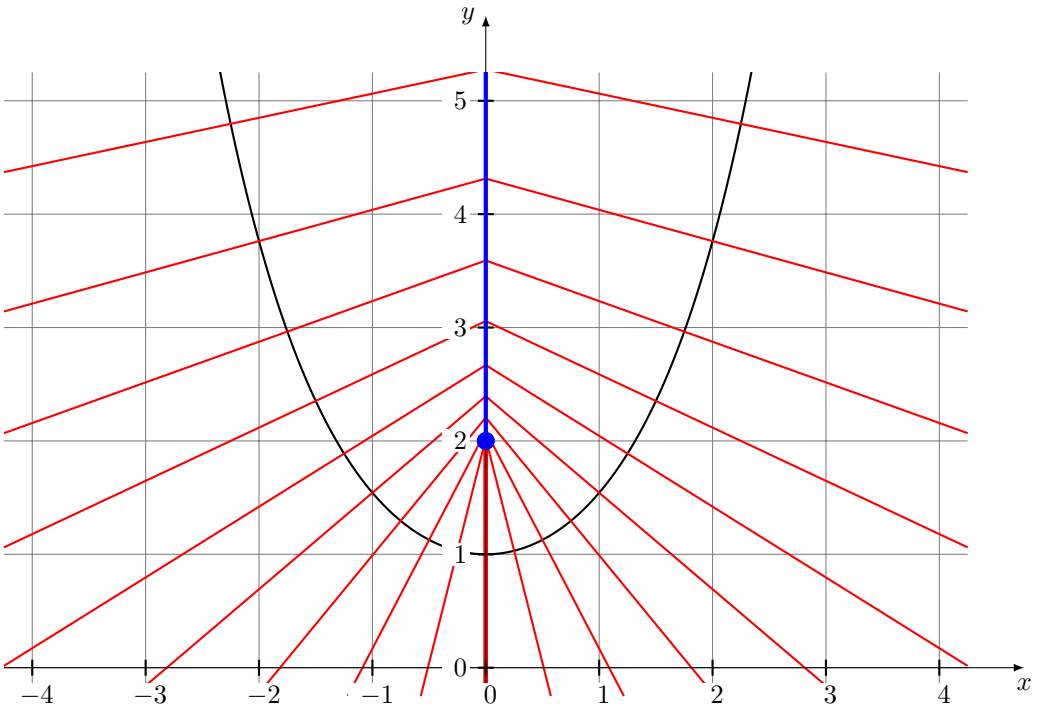


Figure 2: The relationship between the points and the closest points on the catenary curve. The black line is a catenary curve; the red lines are normal lines to the catenary curve; the blue line is where two points on the catenary curve have the same distance; and the blue dot is an area of instability for finding the closest point on the catenary curve.

In the next step, using the found partition, the approximate location for the closest point is found by maintaining the same proportion of distances between the points and the region bounds. See Figure 3, for the point $\mathbf{p}$, the distances are measured as the shortest distances to the region's bounds. For the point on the catenary curve $\mathbf{p}_c$, the distances are measured along the catenary curve to the region's bounds. Therefore,

$$\frac{\rho(\mathbf{p}'_a, \mathbf{p}')}{\rho(\mathbf{p}'_a, \mathbf{p}'_b)} = \frac{\mathrm{d}(\mathbf{p}_a, \mathbf{p})}{\mathrm{d}(\mathbf{p}_a, \mathbf{p}) + \mathrm{d}(\mathbf{p}, \mathbf{p}_b)},$$

where $\rho(\mathbf{p}_0, \mathbf{p}_1) = |\sinh(x_1) - \sinh(x_0)|$ is the distance along the catenary curve between points $\mathbf{p}_0 = \begin{bmatrix} x_0 \\ \cosh(x_0) \end{bmatrix}$ and $\mathbf{p}_1 = \begin{bmatrix} x_1 \\ \cosh(x_1) \end{bmatrix}$; and $\mathrm{d}(\mathbf{p}_0, \mathbf{p}_1)$ is the Euclidean distance between points $\mathbf{p}_0$ and $\mathbf{p}_1$.[2]

In the final step of finding the closest point, we will use an iterative algorithm. We consider two approximations: one by the osculating parabola, and another by the osculating circle.

A. Approximation by the Osculating Parabola

In point $\mathbf{p}_c = \begin{bmatrix} x_c \\ y_c \end{bmatrix}$, where $y_c = \cosh(x_c)$, we will approximate the catenary curve as an osculating parabola; see Figure 4. The equation for the osculating parabola is $y(x) = \cosh(x_c) + \sinh(x_c) \cdot (x - x_c) + \frac{1}{2} \cdot \cosh(x_c) \cdot (x - x_c)^2$. The next step is to find the projection of point $\mathbf{p}$ onto the osculating parabola. The projected point $\mathbf{p}'$ will satisfy

$$(\mathbf{p} - \mathbf{p}') \perp \mathbf{d}',$$

where

$$\mathbf{p}' = \begin{bmatrix} x_c + \Delta x \\ \cosh(x_c) + \sinh(x_c) \cdot \Delta x + \frac{1}{2} \cdot \cosh(x_c) \cdot \Delta x^2 \end{bmatrix}$$

and

$$\mathbf{d}' = \begin{bmatrix} 1 \\ \sinh(x_c) + \cosh(x_c) \cdot \Delta x \end{bmatrix}$$

[2]Because partitioning lines change directions, they are not parallel and, therefore, will intersect. Another way to find an approximate location of the closest point is by evaluating proportion from formed angles. This approach is less robust for larger values of x.

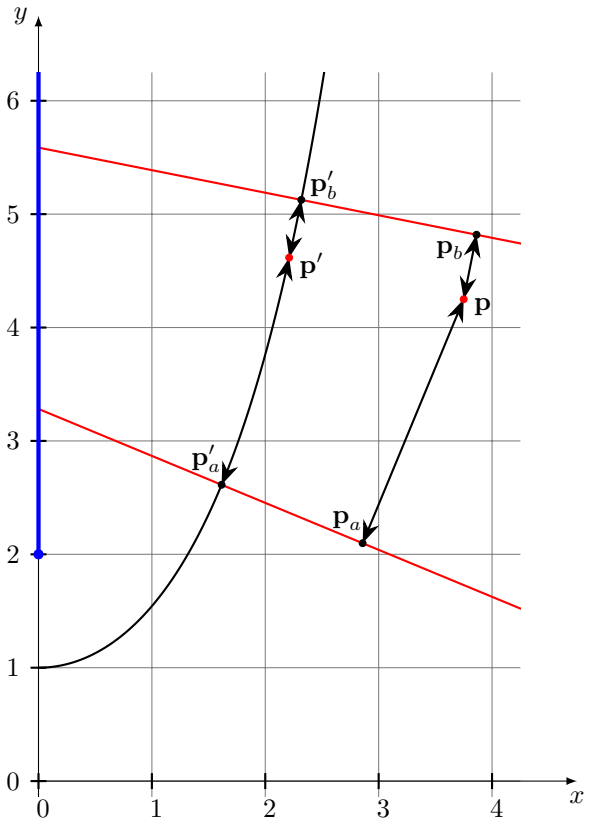


Figure 3: Example of partitioning by normal lines to the catenary curves (red lines) at points $\mathbf{p}'_a$ and $\mathbf{p}'_b$. $\mathbf{p}_a$ and $\mathbf{p}_b$ are the points on these normal lines closest to the point $\mathbf{p}$. $\mathbf{p}'$ approximates the point closest to the point $\mathbf{p}$ on the catenary curve. See the text for details.

is the tangent vector to the parabola at point $\mathbf{p}'$.

Measuring the distance from point $\mathbf{p}_c$ to $\mathbf{p}'$ along the parabola (see Appendix II) and finding point $\mathbf{p}_1$ on the same distance from point $\mathbf{p}_c$ measured on the catenary curve will produce the next approximation of the closest point on the catenary curve.

Two vectors are orthogonal if—and only if—their scalar product is zero; therefore,

$$-\frac{1}{2}\cdot\cosh^2(x_c)\cdot\Delta x^3-\frac{3}{2}\cdot\cosh(x_c)\cdot\sinh(x_c)\cdot\Delta x^2-\left(\cosh^2(x_c)-(y_p-y_c)\cdot\cosh(x_c)\right)\cdot\Delta x+$$
$$+\left((x_p-x_c)+(y_p-y_c)\cdot\sinh(x_c)\right)=0.$$

Dividing this equation by $-\frac{1}{2}\cdot\cosh^2(x_c)$ produces

$$\begin{aligned}&\Delta x^3+3\cdot\tanh(x_c)\cdot\Delta x^2+2\cdot(2-y_p\cdot\operatorname{sech}(x_c))\cdot\Delta x+\\&+2\cdot\left((x_c-x_p)\cdot\operatorname{sech}^2(x_c)+(1-y_p\cdot\operatorname{sech}(x_c))\cdot\tanh(x_c)\right)=0.\end{aligned}\tag{4}$$

Cubic equations with real coefficients can only have either one or three real roots. Without loss of generality, it is assumed that $x_p>0$. It can be shown that if there are three roots, the closest point on the parabola will correspond to the largest root; see Appendix III for details.

Taking the solution of the cubic equation from [14, chapter 5.6], it follows that

$$\Delta x^3+3\cdot a'\cdot\Delta x^2+2\cdot b'\cdot\Delta x+2\cdot c'=0,$$

where

$$\begin{aligned}a'&=\tanh(x_c),\\b'&=(2-y_p\cdot\operatorname{sech}(x_c)),\text{ and}\\c'&=(x_c-x_p)\cdot\operatorname{sech}^2(x_c)+(1-y_p\cdot\operatorname{sech}(x_c))\cdot\tanh(x_c).\end{aligned}$$

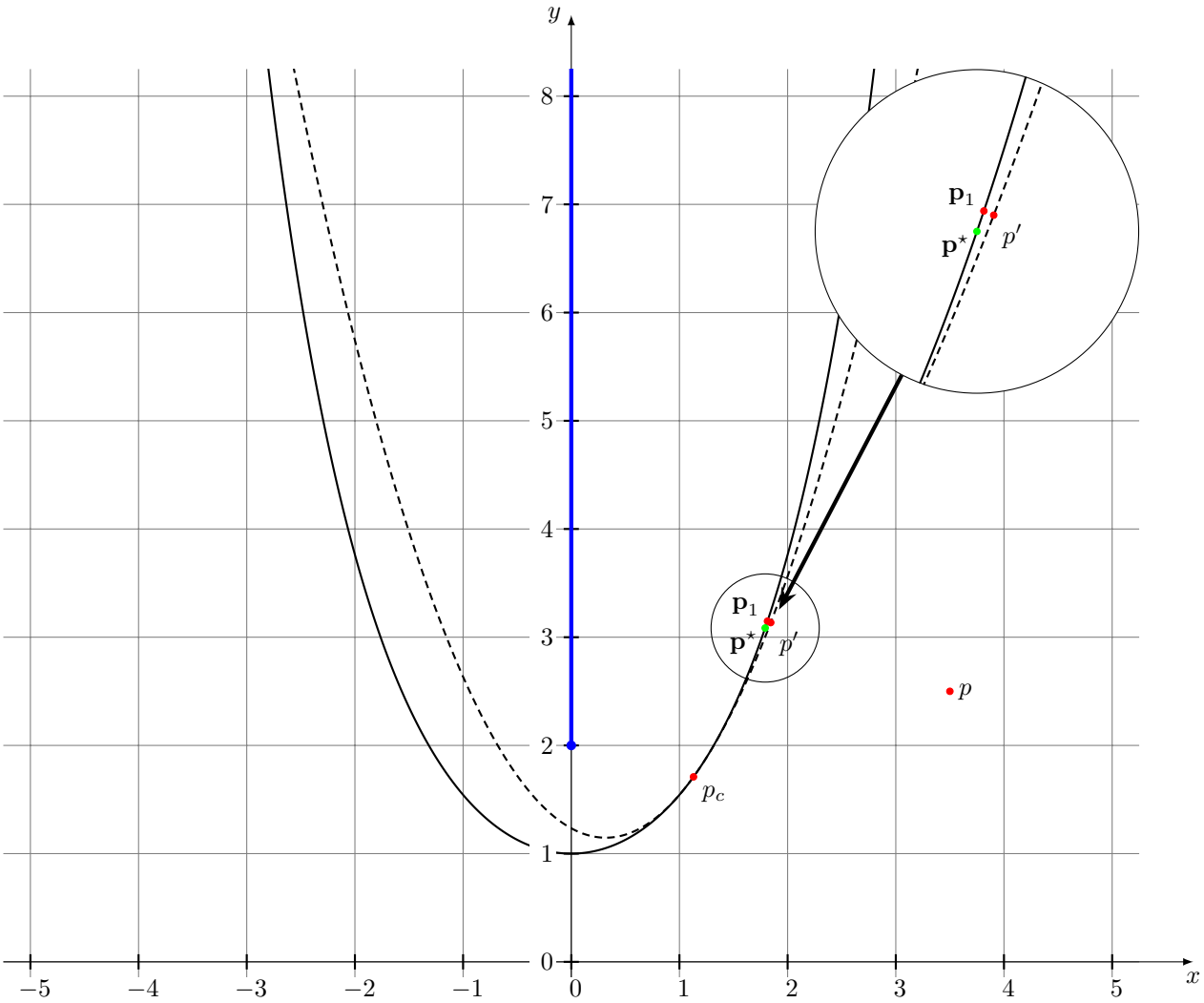


Figure 4: Approximation of a catenary curve (black line) by a parabola (dashed line) at the point $\mathbf{p}_c$. This represents one step of the algorithm for finding the closest point on the catenary curve for the point $\mathbf{p}$ as point $\mathbf{p}_1$. The point $\mathbf{p}'$ is the projection of the point $\mathbf{p}$ onto the parabola. The point $\mathbf{p}_1$ is found to have the same distance along the catenary curve as the point $\mathbf{p}'$ along the parabola from the point $\mathbf{p}_c$. $\mathbf{p}^\star$ is the point on the catenary curve closest to the point $\mathbf{p}$.

$$Q = a'^2 - \frac{2}{3}b',$$
$$R = a'^3 - a' \cdot b' + \frac{1}{2}c'.$$

If $R^2 < Q^3$ the largest root is

$$\Delta x = 2 \cdot \sqrt{Q} \cdot \cos\left(\frac{\Theta}{3}\right) - a',$$

where $\Theta = \arccos\left(-\frac{R}{Q^{\frac{3}{2}}}\right)$; otherwise,

$$\Delta x = (A + B) - a',$$

where

$$A = -\operatorname{sign}(R) \cdot \left(|R| + \sqrt{R^2 - Q^3}\right)^{\frac{1}{3}},$$

$$B = \begin{cases} \dfrac{Q}{A}, & \text{if } A \neq 0; \\ 0, & \text{otherwise.} \end{cases}$$

Due to a round off error, the found correction Δx can be significantly off, requiring some iterative algorithm to improve precision of the solution for the cubic equation; see [14, chapter 9.5]. Applying Laguerre's method [14, chapter 9.5.3] produces good results.

B. Approximation by the Osculating Circle

In point $\mathbf{p}_c = \begin{bmatrix} x_c \\ y_c \end{bmatrix}$, where $y_c = \cosh(x_c)$, we will approximate the catenary curve as an osculating circle; see Figure 5. The osculating circle will have the radius $\cosh^2(x_c)$ and center at $\begin{bmatrix} x_c - \sinh(x_c) \cdot \cosh(x_c) \\ y_c + \cosh(x_c) \end{bmatrix}$. [3] Point $\mathbf{p}'$ is the projection of point $\mathbf{p}$ onto the osculating circle. Measuring the distance on the circle from point $\mathbf{p}_c$ to $\mathbf{p}'$ and finding point $\mathbf{p}_1$ at the same distance from point $\mathbf{p}_c$ measured on the catenary curve will produce the next approximation of the closest point on the catenary curve.

Let $\mathbf{p}_c = \begin{bmatrix} x_c \\ \cosh(x_c) \end{bmatrix}$ be the current approximation of the point closest to the point $\mathbf{p}$. The normal vector to the catenary curve at the point $\mathbf{p}_c$ will be $v_n = (x_n, y_n) = (\tanh(x_c), -\operatorname{sech}(x_c))$. Rotate vector $\mathbf{p} - \mathbf{p}_c$ in the opposite direction of vector v_n. This should rotate vector $\mathbf{v}_n$ to $\begin{bmatrix} 1 \\ 0 \end{bmatrix}$.

$$\mathbf{v}_r = \begin{bmatrix} x_r \\ y_r \end{bmatrix} = \begin{bmatrix} x_n & y_n \\ -y_n & x_n \end{bmatrix} \cdot (p - p_c).$$

The radius of the osculating circle is

$$r = \cosh^2(x_c).$$

The chordal distance between $\mathbf{p}_c$ and $\mathbf{p}'$ is

$$l_c = \sqrt{\left(r \cdot \left(\frac{1}{\sqrt{\left(1 + \left(\frac{y_r}{r + x_r}\right)^2\right)}} - 1 \right)\right)^2 + \left(\frac{y_r}{\sqrt{\left(1 + \frac{x_r}{r}\right)^2 + \left(\frac{y_r}{r}\right)^2}} \right)^2}.$$

In this equation, dividing first by $r + x_r$ and r improves the stability of the numeric evaluation.

$$l = \begin{cases} 2 \cdot r \cdot \arcsin\left(\dfrac{l_c}{2 \cdot r}\right), & \text{if } 2.149\,119\,332\,890\,820\,95 \times 10^{-8} < \dfrac{l_c}{2 \cdot r}; \\ l_c, & \text{otherwise.} \end{cases}$$

In this equation, to prevent underflow, the constant $2.149\,119\,332\,890\,820\,95 \times 10^{-8}$ was used to skip evaluation of arcsin for small values. This constant is the largest number for which arcsin does not modify the number; however, it depends on the implementation of the arcsin function. In the case where r overflows, $l = |y_r|$.

Taking the distance l in the direction of y_r from point $\mathbf{p}_c$ along the catenary curve will yield point $\mathbf{p}_1$, which is the next approximation for the point on the catenary curve closest to point $\mathbf{p}$.

C. Choice for the Approximation Algorithm

Both approximation algorithms work well and can be used to find the closest point on the catenary curve. While approximating by the osculating parabola produces a more precise solution than using the osculating circle, the latter produces a faster solution. About three iterations are sufficient to reach a relative precision of 10^{-6}.

[3] Notice that the x-coordinate of the osculating circle center is of the opposite sign of x_c unless x_c is equal to 0; and the y-coordinate is always twice the y_c.

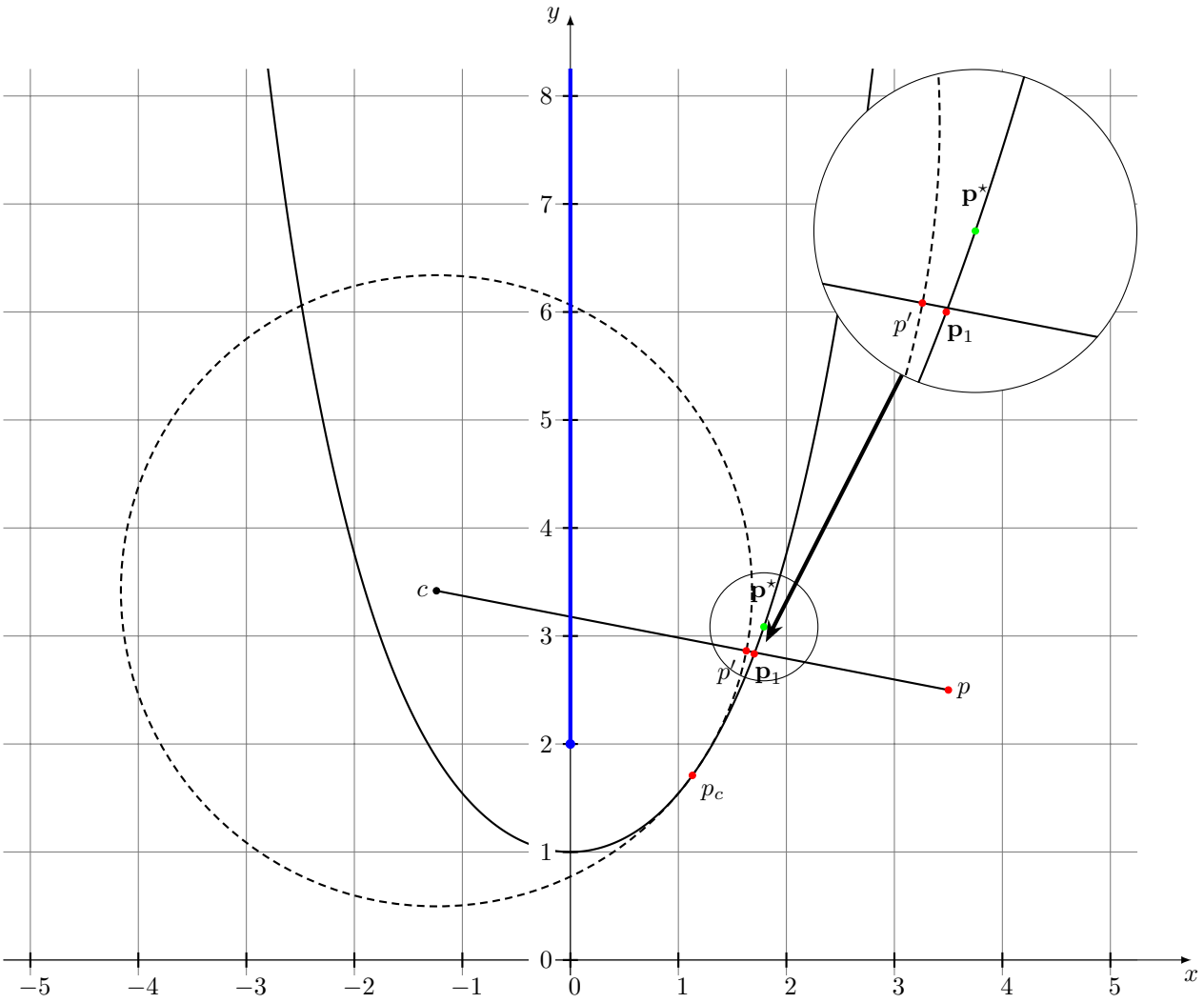


Figure 5: Approximation of a catenary curve (black line) by an osculating circle (dashed line) at the point $\mathbf{p}_c$. This represents one step of the algorithm for finding the closest point on the catenary curve for the point $\mathbf{p}$ as point $\mathbf{p}_1$. The point $\mathbf{p}'$ is the projection of the point $\mathbf{p}$ onto the osculating circle. The point $\mathbf{p}_1$ is found to have the same distance along the catenary curve as the point $\mathbf{p}'$ along the circle from the point $\mathbf{p}_c$. The point $\mathbf{p}^\star$ is the location on the catenary curve closest to the point $\mathbf{p}$.

V. Fitting a Catenary Curve to Points

In the previous section, the task of finding the closest point on the catenary curve was solved. This section will describe the algorithm for fitting a catenary curve to a set of points using a nonlinear least squares algorithm where the parameters of the curve are optimized to minimize the sum of minimum distances between the source points and the curve.

Let's define a signed distance from a point $\mathbf{p} = \begin{bmatrix} x_p \\ y_p \end{bmatrix}$ to the catenary curve as a scalar product of the normal to the catenary curve at the point $\mathbf{p}_c$ and $\overrightarrow{\mathbf{p}_c, \mathbf{p}}$,

$$F(c, a, m|\mathbf{p}, \mathbf{p}_c) = \left(\tanh\left(\frac{x_c - m}{a}\right), -\operatorname{sech}\left(\frac{x_c - m}{a}\right)\right) \cdot \left(x_p - x_c, y_p - \left(c + a \cdot \cosh\left(\frac{x_c - m}{a}\right)\right)\right),$$

where $\mathbf{p}_c = \begin{bmatrix} x_c \\ y_c \end{bmatrix}$, $y_c = c + a \cdot \cosh\left(\frac{x_c - m}{a}\right)$, is the point on the catenary curve closest to $\mathbf{p}$. Point $\mathbf{p}_c$ is found using the algorithm described in Section IV.

This equation will be used in the trust region algorithm [15]–[19] to find optimal parameters c, a, and m by minimizing the sum of $\left\|F\left(c,a,m|\mathbf{p}_i,\mathbf{p}_{c,i}\right)\right\|^2$ over a set of points $\mathbf{p}_i$, where $\mathbf{p}_{c,i}$ is the point on the catenary curve closest to the point $\mathbf{p}_i$. The algorithm requires an evaluation of the function and its first derivatives,

$$
\begin{aligned}
F(c,a,m|p,p_c) &= a + \operatorname{sech}\left(\frac{x_c-m}{a}\right)\cdot\left((x_p-x_c)\cdot\sinh\left(\frac{x_c-m}{a}\right)-(y_p-c)\right),\\
F'_c(c,a,m|p,p_c) &= \operatorname{sech}\left(\frac{x_c-m}{a}\right),\\
F'_a(c,a,m|p,p_c) &= \frac{x_c-m}{a}\cdot F'_m(c,a,m|p,p_c)+1,\\
F'_m(c,a,m|p,p_c) &= -\frac{\operatorname{sech}^2\left(\frac{x_c-m}{a}\right)\cdot\left((y_p-c)\cdot\sinh\left(\frac{x_c-m}{a}\right)+(x_p-x_c)\right)}{a}.
\end{aligned}
$$

While the x-coordinate of the closest point location is not moving when catenary curve parameters change, the scalar product to the normal keeps only the orthogonal distance to the linear approximation at location $\mathbf{p}_c$; see examples in Figure 6. This approach is essentially a linear approximation compared to the distance calculated using the fixed point on the catenary curve.

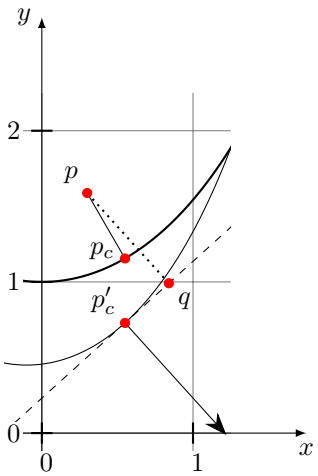


Figure 6: Example of approximation of the shortest distance from the point to the catenary curve when the catenary curve is moving. The distance from the point $\mathbf{p}$ to the catenary curve (thin black line) is approximated as the shortest distance $\overrightarrow{\mathbf{p},\mathbf{q}}$ (dotted line) to the tangent line (dashed line) constructed at the point on the catenary curve $\mathbf{p}'_c$. That distance can be found as the absolute value of the scalar product of the normal to the catenary curve at point $\mathbf{p}'_c$ and $\overrightarrow{\mathbf{p},\mathbf{p}'_c}$. The point $\mathbf{p}'_c$ on the catenary curve is found to have the same x-coordinate as the point $\mathbf{p}_c$ on the source catenary curve (thick black line) closest to the point $\mathbf{p}$.

The domain of parameter a is $(0;+\inf)$. To apply the trust region algorithm without constraint, we will make the following substitution: $a = e^{a_e}$. The first derivative for a_e is

$$F'_{a_e}(c,e^{a_e},m|\mathbf{p},\mathbf{p}_c) = F'_a(c,e^{a_e},m|\mathbf{p},\mathbf{p}_c)\cdot e^{a_e}.$$

The steps of the algorithm are the following:

1. Find the vertical plane that best fits the original points in terms of the least squares distance from the plane.
2. Define a coordinate system on the fitted plane with the x-axis being horizontal and the y-axis being vertical. The x-axis can be found by projecting the normal vector to the horizontal plane, normalizing it, and rotating clockwise by 90 degrees. The y-axis can be found by the vector product of the normal and the found x-axis direction.
3. Project source points onto the plane. Let projected points be $\mathbf{p}_i = \begin{bmatrix} x_i \\ y_i \end{bmatrix}$, where $i = \overline{1..n}$, and n is the number of points.
4. Fit the parabola to the points.
5. Check if the parabola is close to the straight line or concave. If it is, the catenary curve does not represent the points.

6. Find the center of mass for the projected points.
7. Find the closest point on the parabola for the found center. It is done through solving a cubic equation; see [14] and Section IV-A.
8. Find catenary curve parameters a_0 and m_0 by matching the first and second derivatives of the catenary curve at the closest point on the parabola. The parameter c_0 is found to minimize the sum of squared deviations between the catenary curve and the data (average difference between the points and the catenary curve). This will produce initial estimates for catenary curve parameters c_0, a_0, and m_0.
9. Apply the trust region algorithm.[4]

We have noticed that some power lines captured in lidar surveys are slightly rotated by the wind. In such cases, in step 1, the optimal plane's orientation can be found to account for the influence of the wind in lieu of fitting to a vertical plane. We assume that the wind blows in one direction with consistent strength.[5]

This algorithm is applied to real data that often contains outliers introduced by the following:

- Sensor noise producing improper points during the lidar survey
- Misclassified points that do not belong to any catenary curve
- Points from a different catenary curve during the clustering process

For these reasons, it became necessary to provide a user-specified maximum deviation threshold from the catenary curve that can be tailored to the data being processed. To make this algorithm robust to outliers, points exceeding this threshold need to be removed, and the algorithm needs to be reapplied to the remaining points.

Note that fitting a plane in step 1 does not find the optimal plane for the catenary curve but rather a close approximation. Finding an optimal plane requires simultaneous optimization of parameters for the catenary curve and the plane.

VI. Example

This solution can be demonstrated using a lidar survey collected over Utrecht, the Netherlands [1], which captures a series of transmission power lines. The points representing power lines were labeled using a PointCNN classification model; see Figure 7a. Line features modeling each power line's catenary curve were obtained by using the Extract Power Lines From Point Cloud tool in ArcGIS Pro [20], which implemented the solution discussed in this paper.

1. The Extract Power Lines From Point Cloud tool was executed with the following parameters:
   - Power line class code: 14
   - Point tolerance: 80 cm
   - Wire separation distance: 1 m
   - Maximum wire sampling gap: 15 m
   - Output line tolerance: 1 cm
   - Minimum span for wind correction: 60 m
   - Maximum deviation angle: 10°
   - End point search radius: 10 m
   - Minimum wire length: 5 m
2. The tool generated a unique catenary curve for each power line; see Figure 7b.
3. The resultant power line was used to create a surface modeling a 15-meter horizontal clearance from the outermost power lines and a 9-meter vertical clearance from the lowest power lines; see Figure 7c.
4. This clearance surface was then used alongside a surface model of vegetation cover to evaluate the volume and area of the trees that exceed the clearance surface; see Figure 7d. These results provide a basis for determining the quantity of vegetation that has exceeded the clearance zone.

The aforementioned example demonstrates how the solution presented in this paper can be used to extract power lines as part of a downstream application for evaluating vegetation encroachment.

VII. Conclusion

This paper describes a solution for accurately extracting unique catenary curves from an array of points representing multiple catenary curves. The solution can be used to extract power lines from lidar surveys to support downstream applications. An example illustrating the potential use of this solution was provided in the examination of vegetation encroachment around transmission power lines.

[4]Note that the result of this algorithm does not depend on the distance of the points to the fitted catenary curve plane (projection plane) because the squared distance to any point on the projection plane is the sum of the squared distance to the projection plane and the squared distance from the projected point to that point. However, squared distances from the points to the projection plane are fixed.

[5]Strong or inconsistent winds acting on a long power line can produce irregular distortions of its shape that create noncatenary curves. No examples of this were discovered when surveying available data for power lines and therefore were not considered in this paper.

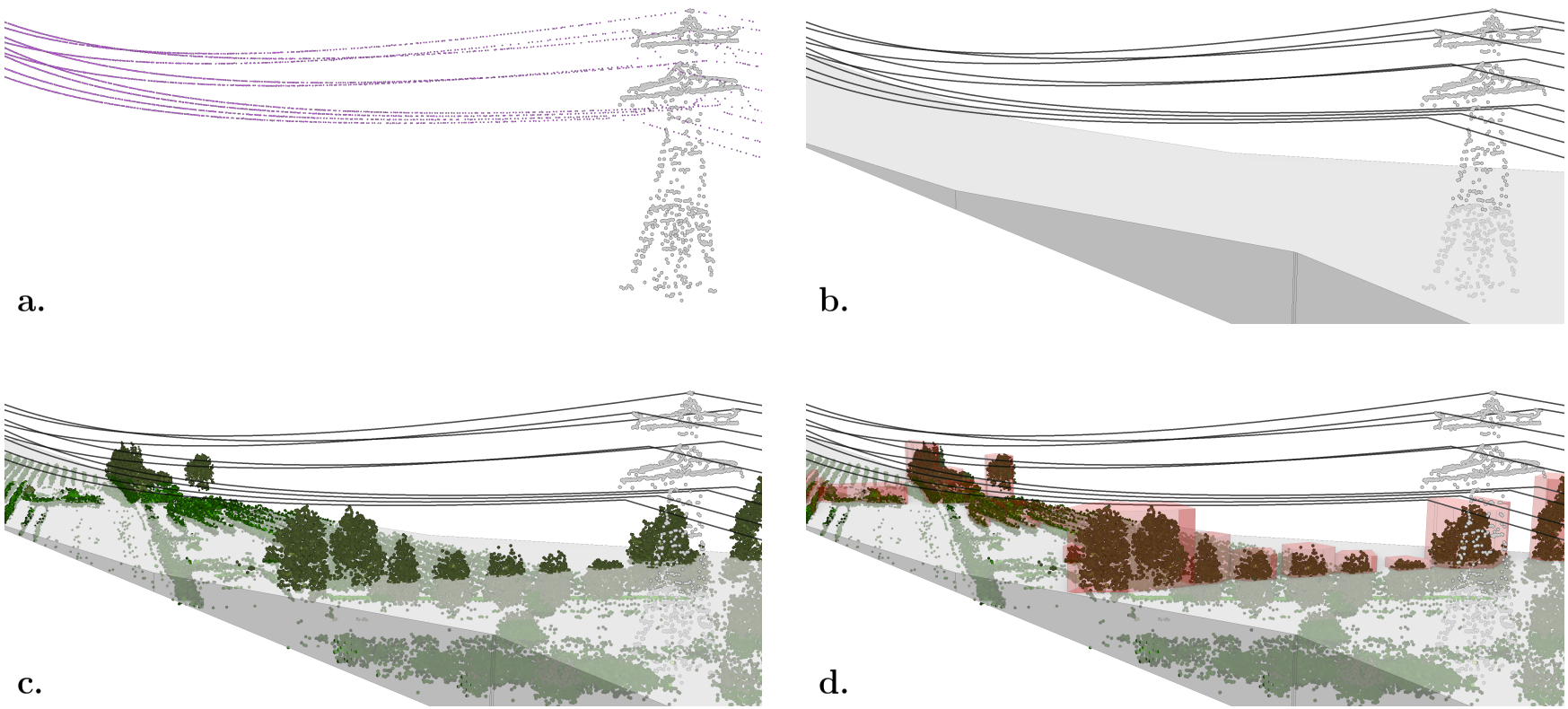


Figure 7: Screenshots of results obtained in ArcGIS Pro when applying the catenary curve modeling solution to a workflow for managing vegetation growth around power lines.

a. Lidar points classified as power lines are drawn in purple, and transmission towers are drawn in gray.
b. This screenshot shows line features constructed from the power line classified points and the clearance surface constructed from the line features.
c. Vegetation points are displayed against a semitransparent clearance surface. Vegetation points within the clearance surface are tinted gray.
d. Vegetation points exceeding the clearance surface are enclosed within a red bounding box.

Also in this paper, a new, efficient algorithm to find the closest point on the catenary curve is introduced, along with a new algorithm for fitting a catenary curve to a set of points based on the shortest distance. This algorithm fits a catenary curve to points by approximating the shortest distance as a scalar product of a normal and the vector; see Section V. Such an approach provides a general framework that can be applied to fitting other curves. The clustering algorithm is based on a minimum spanning tree, a dynamic programming approach, and the k-mean clustering technique.

Acknowledgments

The authors would like to thank Lois Stuart and Linda Thomas for proofreading this paper; and Manoj Lnu, senior software engineer, 3D analyst at Esri, for helpful discussions about the initial fitting of a catenary curve to a set of points.

Appendix I. Equation (3)

$$y = \cosh(x) + \frac{x}{\sinh(x)},$$

$$\begin{aligned} y' =& \sinh(x) + \frac{\sinh(x) - x\cosh(x)}{\sinh^2(x)} = \\ =& \frac{\sinh^3(x) + \sinh(x) - x\cosh(x)}{\sinh^2(x)} = \\ =& \frac{\sinh(x)\left(\sinh^2(x) + 1\right) - x\cosh(x)}{\sinh^2(x)} = \\ =& \frac{\sinh(x)\cosh^2(x) - x\cosh(x)}{\sinh^2(x)} = \\ =& \frac{\cosh(x)}{\sinh^2(x)}\left(\sinh(x)\cosh(x) - x\right) = \\ =& \frac{\cosh(x)}{\sinh^2(x)}\left(\frac{\sinh(2x)}{2} - x\right). \end{aligned} \tag{5}$$

Because $\sinh(x) - x$ is a strictly increasing odd function, it follows that (5) is positive for all positive values and negative for all negative values; therefore, (3) is strictly increasing for all positive values and strictly decreasing for all negative values.

The minimum point of the intersection of the y-axis is always above 2, because

$$\lim_{x\to 0}\left(\cosh(x) + \frac{x}{\sinh(x)}\right) = 2.$$

Appendix II. Length along a Parabola

For the parabola

$$y = \frac{1}{2}x^2 \tag{6}$$

the length from point $\begin{bmatrix}0\\0\end{bmatrix}$ to point $\begin{bmatrix}x\\\frac{1}{2}x^2\end{bmatrix}$ is calculated as the next integral

$$\mathrm{L}(x) = \int_0^x \sqrt{1+t^2}\cdot dt.$$

The solution for this integral can be found in [21, p. 225, eq. 42].

$$\int \sqrt{x^2+a^2}\cdot dx = \frac{x}{2}\sqrt{x^2+a^2} + \frac{a^2}{2}\log\left|x + \sqrt{x^2+a^2}\right| + C,$$

where C is an arbitrary constant.

Taking $a = 1$ and replacing x with an absolute value of x to stabilize the evaluation of this integral for negative values (see the note on the evaluation of arcsinh in [14, chapter 5.6]), we obtain

$$\mathrm{L}(x) = \operatorname{sign}(x) \cdot \frac{|x| \cdot \sqrt{x^2+1} + \log\left(|x| + \sqrt{x^2+1}\right)}{2}. \tag{7}$$

Therefore, the length along any parabola

$$y = a \cdot x^2 + b \cdot x + c$$

between x_0 and x_1 can be found by shifting and scaling to match the parabola defined in (6). Using (7), we obtain

$$\mathrm{L}(x_0, x_1, a, b) = \frac{L(2 \cdot a \cdot x_1 + b) - L(2 \cdot a \cdot x_0 + b)}{2 \cdot a}.$$

Appendix III. On the Roots of the Cubic Equation (4)

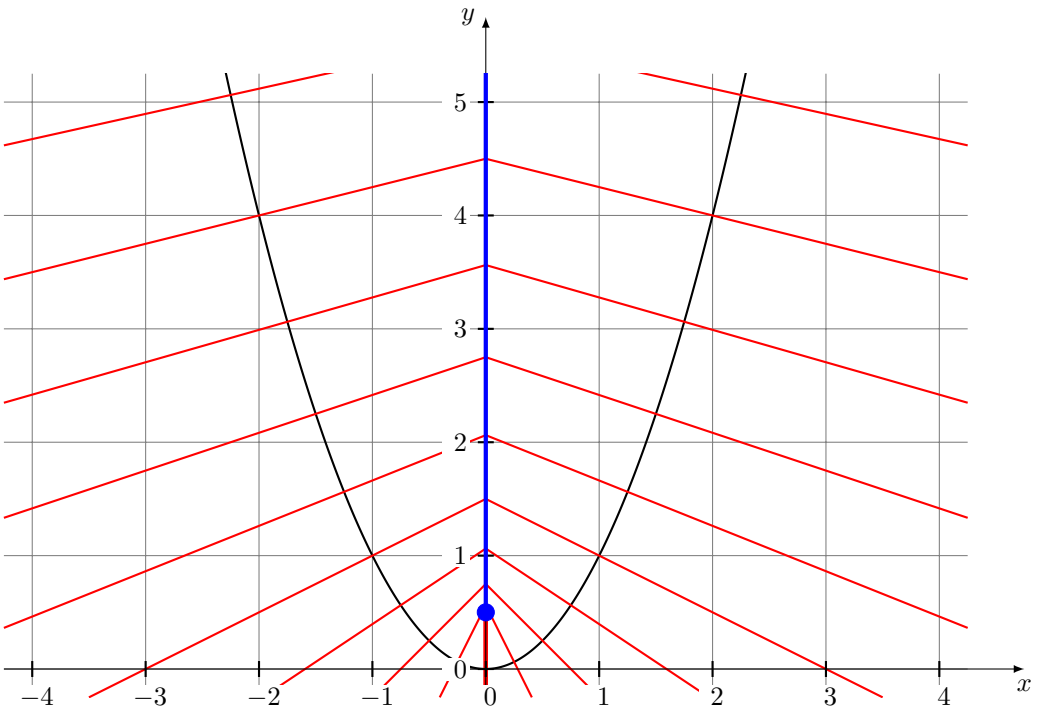


Figure 8: The relationship between the points and the closest points on the parabola ($y = x^2$). The black line is a parabola; the red lines are normal lines to the parabola; the blue line is where two points on the catenary curve have the same distance; and the blue dot is an area of instability for finding the closest point on the parabola.

Figure 8, like Figure 2, shows the relationship between the points and the closest position on the parabola. This relationship holds for different parabola shapes.

Let's define a parabola as

$$y = a \cdot x^2,$$

where $a > 0$ is a coefficient. The normal line will intersect the y-axis at

$$y = a \cdot x^2 + \frac{1}{2 \cdot a}.$$

From this, it follows that the normal lines constructed for the points on the parabola for half-plane $x > 0$ do not intersect in this half-plane. It is the same as for the catenary curve. Therefore, there is only one closest point for points in the half-plane. Also, it follows that if there are three real roots for the cubic equation for points in the half-plane, two of them are negative and one is positive. For our task, we should only consider finding the closest point on the parabola's right branch because the left side of the parabola is not a good approximation of the catenary curve. Therefore, when looking for the closest point on the parabola and the point is located in another half-plane $x \leq 0$, there might be several positive roots, but the one with the largest value will be used.

References

[1] AHN3 downloads. Actueel Hoogtebestand Nederland (current height file, Netherlands). [Online]. Available: https://app.pdok.nl/ahn3-downloadpage/

[2] A. Hatibovic, "Derivation of equations for conductor and sag curves of an overhead line based on a given catenary constant," *Periodica Polytechnica Electrical Engineering and Computer Science*, vol. 58, no. 1, pp. 23–27, 2014. [Online]. Available: https://doi.org/10.3311/PPee.6993

[3] 2020 Wildfire Activity Statistics. California Department of Forestry and Fire Protection. [Online]. Available: https://www.fire.ca.gov/media/0fdfj2h1/2020_redbook_final.pdf

[4] 2019 Wildfire Activity Statistics. California Department of Forestry and Fire Protection. [Online]. Available: https://www.fire.ca.gov/media/iy1gpp2s/2019_redbook_final.pdf

[5] 2018 Wildfire Activity Statistics. California Department of Forestry and Fire Protection. [Online]. Available: https://www.fire.ca.gov/media/11146/2018_redbook_final.pdf

[6] 2017 Wildfire Activity Statistics. California Department of Forestry and Fire Protection. [Online]. Available: https://www.fire.ca.gov/media/10059/2017_redbook_final.pdf

[7] Otakar Borůvka, "O jistém problému minimálním," *Práce Moravské přírodovědecké společnosti*, vol. III, no. 3, pp. 37–58, 1926, Czech, German summary. [Online]. Available: http://hdl.handle.net/10338.dmlcz/500114

[8] ——, "Příspěvek k otázce ekonomické stavby elektrovodných sítí," *Elektrotechnický obzor*, vol. 15, pp. 153–154, 1926, Czech, German summary. [Online]. Available: http://hdl.handle.net/10338.dmlcz/500188

[9] J. B. Kruskal, "On the shortest spanning subtree of a graph and the traveling salesman problem," *Proceedings of the American Mathematical Society*, vol. 7, no. 1, pp. 48–50, 1956. [Online]. Available: https://doi.org/10.1090/S0002-9939-1956-0078686-7

[10] R. C. Prim, "Shortest connection networks and some generalizations," *The Bell System Technical Journal*, vol. 36, no. 6, pp. 1389–1401, 1957. [Online]. Available: https://doi.org/10.1002/j.1538-7305.1957.tb01515.x

[11] J. Nešetřil, E. Milková, and H. Nešetřilová, "Otakar Borůvka on minimum spanning tree problem. Translation of both the 1926 papers, comments, history," *Discrete Mathematics*, vol. 233, no. 1-3, pp. 3–36, 2001, Czech and Slovak 2. [Online]. Available: https://doi.org/10.1016/S0012-365X(00)00224-7

[12] H.-H. Bock, "Origins and extensions of the k-means algorithm in cluster analysis," *Journal Electronique d'Histoire des Probabilités et de la Statistique / Electronic Journal for History of Probability and Statistics*, vol. 4, no. 2, pp. 1–18, December 2008. [Online]. Available: http://www.jehps.net/Decembre2008/Bock.pdf

[13] A. Gribov and E. Bodansky, "A new method of polyline approximation," in *Structural, Syntactic, and Statistical Pattern Recognition*, ser. Lecture Notes in Computer Science, A. Fred, T. M. Caelli, R. P. Duin, A. Campilho, and D. de Ridder, Eds. Springer Berlin Heidelberg, 2004, vol. 3138, pp. 504–511. [Online]. Available: https://doi.org/10.1007/978-3-540-27868-9_54

[14] W. H. Press, S. A. Teukolsky, W. T. Vetterling, and B. P. Flannery, *Numerical Recipes, Third Edition: The Art of Scientific Computing*. Cambridge University Press, 2007. [Online]. Available: www.cambridge.org/9780521880688

[15] A. R. Conn, N. I. M. Gould, and P. L. Toint, *Trust Region Methods*. Society for Industrial and Applied Mathematics, 2000. [Online]. Available: https://doi.org/10.1137/1.9780898719857

[16] K. Levenberg, "A method for the solution of certain non-linear problems in least squares," *Quarterly of Applied Mathematics*, vol. 2, pp. 164–168, 1944. [Online]. Available: https://doi.org/10.1090/qam/10666

[17] D. W. Marquardt, "An algorithm for least-squares estimation of nonlinear parameters," *Journal of the Society for Industrial and Applied Mathematics*, vol. 11, no. 2, pp. 431–441, 1963. [Online]. Available: https://doi.org/10.1137/0111030

[18] A. Ranganathan. (2004) The Levenberg-Marquardt algorithm. [Online]. Available: http://www.ananth.in/Notes_files/lmtut.pdf

[19] H. P. Gavin. (2020) The Levenberg-Marquardt method for nonlinear least squares curve-fitting problems. [Online]. Available: https://people.duke.edu/~hpgavin/ce281/lm.pdf

[20] Extract power lines from point cloud (3D Analyst). Retrieved October, 2021. [Online]. Available: pro.arcgis.com/en/pro-app/latest/tool-reference/3d-analyst/extract-power-lines-from-point-cloud.htm

[21] В. Т. Воднев, А. Ф. Наумович, and Н. Ф. Наумович, *Основные математические формулы (Main mathematical formulas)*, Ю. С. Богданова, Ed. Минск, Вышэйшая Школа, 1980.